euronoise 2021
25th to 27th of October
Madeira, Portugal - online

A 2D waveguide to measure oblique incidence reflection and transmission coefficients

Ze Zhang[1,3], Hervé Denayer[1,3], Claus Claeys[1,3], Wim Desmet[1,3], Elke Deckers[2,3]

[1]*KU Leuven, Dept. of Mechanical Engineering, Celestijnenlaan 300, 3001 Leuven, Belgium E-mail:* ***ze.zhang@kuleuven.be***
[2]*KU Leuven, Campus Diepenbeek, Dept. of Mechanical Engineering, Wetenschapspark 27, 3590 Diepenbeek, Belgium*
[3]*DMMS Lab, Flanders Make, Belgium*

Abstract

This paper presents a method to directly measure reflection and transmission coefficients under oblique incidence in a 2D waveguide. The method is particularly suited for characterizing anisotropic materials, where these oblique properties cannot be readily calculated from their normal incidence counterparts. The method works by decomposing the pressure field within the waveguide into cut-on modes based on measurements of the acoustic pressure at multiple microphone positions. The microphone locations are optimized to improve the robustness of the method. The method is validated using numerical simulations of the waveguide containing an anisotropic metamaterial. An excellent agreement of the metamaterial properties is achieved between applying the measurement methodology to a simulation of the waveguide with the metamaterial samples inside and the directly predicted metamaterial properties in a simulation with idealized assumptions. Furthermore, the designed waveguide is realized and a sample of the metamaterial is measured experimentally. A good match is also observed between the measurement and the predicted properties.

Keywords: modal decomposition, anisotropic material characterization, angle-dependent coefficients

1. Introduction

During the product development stage of noise treatment solutions, various acoustic performance metrics of the design including the oblique incidence reflection coefficient (R_o) and oblique incidence transmission coefficient (T_o) need to be evaluated. R_o and T_o of an isotropic material sample can be calculated from the normal incidence reflection coefficient and transmission coefficient, which are measurable using a standard impedance tube. For anisotropic materials, such as metamaterials, this is not possible due to the anisotropy. This implies that a way to directly measure R_o and T_o is needed.

Multiple methods have been proposed to achieve this goal. The free-field in-situ measurement method [1, 2, 3, 4] measures the acoustic field information (e.g., acoustic pressure or sound intensity) around the sample under a known acoustic incidence field. In the post-processing, the reflected field can be separated from the incidence field by analyzing the source and receiver information. However, it requires a large sample and very accurate positioning of the source and receiver throughout the measurements. Moreover, the ability to measure T_o is lacking as the sample is placed on the floor during the measurement which can be regarded as a rigid backing. The spatial Fourier-transform method assumes that the sound field can be decomposed into an infinite series of sinusoidal waves of different propagation directions [5]. By integrating the pressure at an extensive number of points within the field, a sinusoidal wave component of certain propagation angle can be described, which in turn can be used to calculated the reflection coefficient at these incidence angles. Owning to the integration process, acoustic measurements at a large number of points are needed, which yields complex and sometimes intrusive setups [6].

This paper proposes a measurement method based on the modal decomposition method, which assumes the pressure field of a waveguide to be approximated by the summation of cut-on modes [7]. Compared to the previously mentioned methods, it ensures the non-intrusive measurement of both R and T in a setup of an acceptable size. Moreover, after a set of measurements, R_o and T_o under various oblique incidences can be obtained simultaneously.

This paper is organized as follows. Section 2 presents how the modal decomposition method can be used to measure R_o and T_o. Section 3 describes an optimization process for the microphone locations, which

improves the robustness of the method against measurement noise. In section 4, a numerical simulation of the proposed setup with an anisotropic metamaterial is conducted applying the technique from the previous section. Section 4 also discusses the physical realization of the measurement setup and subsequently the measurement results of a metamaterial sample. Finally, the conclusions are given in section 5.

2. From modal decomposition theory to R_o and T_o

This section presents the theories behind the oblique incidence reflection coefficient R_o and transmission coefficient T_o measurements based on the modal decomposition method. Firstly, the field is decomposed into propagating modes using multiple microphone measurements within the waveguide. Secondly, the scattering matrix, i.e., the relationship between the modal amplitudes on both sides of the material sample in a waveguide in matrix form, is calculated from the results of the modal decomposition. Finally, R_o and T_o are calculated from the scattering matrix coefficients.

2.1. Modal decomposition method

The acoustic field inside a waveguide can be described as an infinite sum of duct modes. Each mode describes a certain pattern in the cross-section of the waveguide and has an associated axial wavenumber. For a waveguide with a rectangular cross-section and rigid boundaries as shown in Figure 1, the pressure pattern of mode (m, n) in the cross-section can be expressed as:

$$\Psi^{\pm}_{m,n}(x, y) = C_{m,n} \cos\left(k^x_m x\right) \cos\left(k^y_n y\right), \tag{1}$$

where k^x_m and k^y_n are the wavenumbers of m^{th} mode in the x-direction and the n^{th} mode in the y-direction and $C_{m,n}$ is the scaling factor which is introduced to normalize the acoustic intensity of different duct modes, which is defined as:

$$C_{m,n} = \sqrt{\left(2 - \delta_{m,0}\right)\left(2 - \delta_{n,0}\right)}, \tag{2}$$

where $\delta_{i,j}$ is the Kronecker delta. k^x_m and k^y_n can be expressed as:

$$k^x_m = \frac{m\pi}{W}, \quad k^y_n = \frac{n\pi}{H}, \tag{3}$$

where W and H are shown in Figure 1.

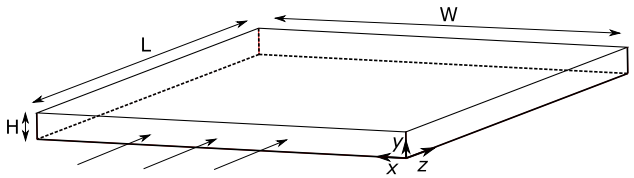

Figure 1: A waveguide with a rectangular cross-section

The axial wavenumber $k^{\pm}_{m,n}$ can be calculated as:

$$k^{\pm}_{m,n} = \sqrt{k^2 - \left(k^x_m\right)^2 - \left(k^y_n\right)^2}, \tag{4}$$

where k is the acoustic wavenumber of sound in air.

The axial wavenumber can be real or imaginary, depending on the frequency, the dimensions of the cross-section and the value of m and n. For a real wavenumber, the mode propagates unattenuated in the axial (z) direction and is called cut-on. An imaginary axial wavenumber represents an evanescent mode which is called cut-off. If sufficiently far from sources and assuming no changes in the cross section, the

acoustic pressure $P(x,y,z)$ at point (x,y,z) inside the waveguide can be approximated as a sum of all cut-on modes [7]:

$$P(x,y,z) \approx \sum_{m,n} \left(P^{+}_{m,n} \Psi^{+}_{m,n}(x,y)\, e^{-jk^{+}_{m,n} z} + P^{-}_{m,n} \Psi^{-}_{m,n}(x,y)\, e^{jk^{-}_{m,n} z} \right), \tag{5}$$

where $P^{\pm}_{m,n}$ is the pressure amplitude of mode (m,n).

For the remainder of this paper, it is assumed that H is sufficiently small to allow only the 0^{th} mode in the y-direction, which leads to $k^y = 0$. The intention of not allowing high-order modes in the y-direction is to make the waveguide essentially two dimensional, which enables non-intrusive measurements since all information needed can be obtained in a single x-z plane. As a result, equation (4) and (5) are rewritten as:

$$k^{\pm}_{m} = \sqrt{k^2 - \left(k^{x}_{m}\right)^2}, \tag{6}$$

and

$$P(x,z) \approx \sum_{m} \left(P^{+}_{m} \Psi^{+}_{m}(x)\, e^{-jk^{+}_{m} z} + P^{-}_{m} \Psi^{-}_{m}(x)\, e^{jk^{-}_{m} z} \right). \tag{7}$$

Equation (7) can be expressed in vector format:

$$P(x,z) \approx \begin{bmatrix} \Psi^{+}_{0}(x)\, e^{-jk^{+}_{0} z} \\ \vdots \\ \Psi^{+}_{N-1}(x)\, e^{-jk^{+}_{N-1} z} \\ \Psi^{-}_{0}(x)\, e^{+jk^{-}_{0} z} \\ \vdots \\ \Psi^{-}_{N-1}(x)\, e^{+jk^{-}_{N-1} z} \end{bmatrix}^{\mathsf{T}} \begin{bmatrix} P^{+}_{0} \\ \vdots \\ P^{+}_{N-1} \\ P^{-}_{0} \\ \vdots \\ P^{-}_{N-1} \end{bmatrix}, \tag{8}$$

where N is the total number of cut-on modes in the x-direction. If s points are measured within the field, equation (8) can be expanded to the matrix form:

$$\begin{bmatrix} P(x_1,z_1) \\ \vdots \\ P(x_s,z_s) \end{bmatrix} \approx \underbrace{\begin{bmatrix} \Psi^{+}_{0}(x_1)\, e^{-jk^{+}_{0} z_1} & \cdots & \Psi^{+}_{0}(x_s)\, e^{-jk^{+}_{0} z_s} \\ \vdots & \vdots & \vdots \\ \Psi^{+}_{N-1}(x_1)\, e^{-jk^{+}_{N-1} z_1} & \cdots & \Psi^{+}_{N-1}(x_s)\, e^{-jk^{+}_{N-1} z_s} \\ \Psi^{-}_{0}(x_1)\, e^{+jk^{-}_{0} z_1} & \cdots & \Psi^{-}_{0}(x_s)\, e^{+jk^{-}_{0} z_s} \\ \vdots & \vdots & \vdots \\ \Psi^{-}_{N-1}(x_1)\, e^{+jk^{-}_{N-1} z_1} & \cdots & \Psi^{-}_{N-1}(x_s)\, e^{+jk^{-}_{N-1} z_s} \end{bmatrix}^{\mathsf{T}}}_{\underline{M}} \underbrace{\begin{bmatrix} P^{+}_{0} \\ \vdots \\ P^{+}_{N-1} \\ P^{-}_{0} \\ \vdots \\ P^{-}_{N-1} \end{bmatrix}}_{\vec{P}}. \tag{9}$$

In case $s \geq 2N$, it is possible that $\operatorname{rank}(\underline{M}) \geq 2N$. In that case, the system of equations (9) is fully or overly determined. $\vec{P}$ can then be calculated as [7]:

$$\vec{P} \approx \underline{M}^{\dagger} \begin{bmatrix} P(x_1,z_1) \\ \vdots \\ P(x_s,z_s) \end{bmatrix}, \tag{10}$$

where $\underline{M}^{\dagger}$ is the pseudo-inverse of $\underline{M}$. This means that by measuring the acoustic pressure at a sufficient number of locations within the field, the field inside the waveguide can be described by a sum of the different cut-on modes with different contributions.

2.2. From modes contribution to the scattering matrix

Based on the modal amplitude of the cut-on modes, the scattering matrix S, which describes the linear acoustic behavior of the material by a matrix relation linking the modal amplitudes on both sides of the sample, can be calculated, as illustrated in figure 2 and equation (11):

$$\left[P^+_{o,0}\cdots P^+_{o,N-1}P^-_{i,0}\cdots P^-_{i,N-1}\right]^\intercal = \underline{S}\left[P^+_{i,0}\cdots P^+_{i,N-1}P^-_{o,0}\cdots P^-_{o,N-1}\right]^\intercal, \tag{11}$$

where $P_i^\pm$ and $P_o^\pm$ are pressure amplitudes on each side.

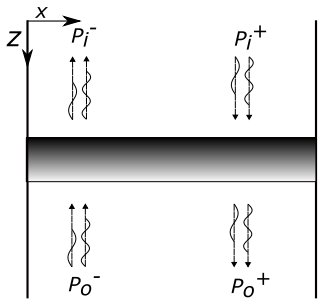

Figure 2: A schematic illustration of wave components propagating into $-z$- and $+z$-directions on both sides of the sample in a wide waveguide

Equation (11) provides $2N$ relations between the $2N$ modal amplitudes of one measurement and the scattering matrix of the system. To fully determine the $(2N)^2$ coefficients of $\underline{S}$, at least $2N$ independent measurements (by varying the position of the excitation and/or the impedance of the termination) at the same microphone locations are needed [7], i.e.:

$$w > 2N, \tag{12}$$

where w is the total number of measurements. This results in a determined or overdetermined system of equations:

$$\underbrace{\begin{bmatrix} P^+_{o,0,1} & \cdots & P^+_{o,0,w} \\ \vdots & & \vdots \\ P^+_{o,N-1,1} & \cdots & P^+_{o,N-1,w} \\ P^-_{i,0,1} & \cdots & P^-_{i,0,u} \\ \vdots & & \vdots \\ P^-_{i,N-1,1} & \cdots & P^-_{i,N-1,w} \end{bmatrix}}_{\underline{P_1}} = \underline{S} \underbrace{\begin{bmatrix} P^+_{i,0,1} & \cdots & P^+_{i,0,w} \\ \vdots & & \vdots \\ P^+_{i,N-1,1} & \cdots & P^+_{i,N-1,w} \\ P^-_{o,0,1} & \cdots & P^-_{o,0,u} \\ \vdots & & \vdots \\ P^-_{o,N-1,1} & \cdots & P^-_{o,N-1,w} \end{bmatrix}}_{\underline{P_2}}, \tag{13}$$

where the second subscript of $P_i^\pm$ and $P_o^\pm$ is a certain mode m in the x-direction and the third subscript denotes a certain measurement. $\underline{S}$ can then be calculated as:

$$\underline{S} = \underline{P_2}^\dagger \underline{P_1}. \tag{14}$$

2.3. From the scattering matrix to R_o and T_o

As mentioned in the previous section, the scattering matrix relation of equation (11) describes the response of the material sample to any combination of incident duct modes. Thus, the scattering matrix coefficients can be interpreted as the transmission and reflection coefficients of an individual incident mode. For example, the response to the m^{th} mode from the top of the material sample is given by the m^{th} row of the scattering matrix, where the first N coefficients describe how this mode is transmitted to different modes on the bottom side of the sample (transmission) and the last N components describe the reflection of

this mode to the different modes propagating back towards the excitation (reflection). As a result, the total fraction of the incident energy which is reflected, transmitted and absorbed by the sample under a positive z-direction m^{th} mode incidence can be calculated as:

$$R_m = \sum_{j=N+1}^{2N} \left(\underline{S}\left(j,m\right)\right)^2, \quad T_m = \sum_{j=1}^{N} \left(\underline{S}\left(j,m\right)\right)^2, \text{ and } \quad \alpha_m = 1 - R_m - T_m, \tag{15}$$

where $\underline{S}\left(j,m\right)$ denotes the j^{th} row and m^{th} column element of $\underline{S}$. From equations (1) and (6) it can be concluded that the m^{th} cut-on mode can be interpreted as an oblique incidence with an incidence angle θ_m:

$$\theta_m = \operatorname{acot}\left(\frac{k_m^{\pm}}{k_m^{x}}\right). \tag{16}$$

Connecting equation (15) and (16), it can be concluded that the response of the material to plane waves under oblique incidence, with an incidence angle corresponding to a cut-on mode can be calculated from the scattering matrix:

$$R_o\left(\theta_m\right) = R_m, \quad T_o\left(\theta_m\right) = T_m, \text{ and } \quad \alpha_o\left(\theta_m\right) = \alpha_m. \tag{17}$$

From equations (1) and (3), it can be concluded that for two ms of the same absolute value but opposite signs (e.g., the 3^{rd} and -3^{rd} modes), the pressure patterns are identical, meaning they can not be differentiated using the modal decomposition method. Thus, neither the two corresponding incidence angles (θ_m and θ_{-m}(i.e., $-\theta_m$)) can be differentiated.

3. Optimization to robustify the measurement results

Looking at equation (10), one can see that the modal matrix $\underline{M}$ needs to be inverted to obtain the modal amplitude, which means that a low condition number of $\underline{M}$ is crucial to ensure an accurate determination of the oblique incidence coefficients. The elements of the modal matrix $\underline{M}$ only depend on the dimensions of the cross-section W and H, the frequency f and the microphone positions (x, z). Therefore, the condition numbers of $\underline{M}$ within a certain frequency range can be improved by optimizing the positions of the microphones [8]. In this section, details of this optimization procedure are presented.

3.1. Determination of waveguide dimensions

First, the dimensions of the waveguide and the frequency range of interest need to be decided. The frequency range is chosen as between 1000 Hz and 3000 Hz since the designed anisotropic metamaterial to be tested is designed specifically for this range. Equation (18) is used to determine the number of available cut-on modes N for a waveguide at frequency f:

$$N\left(f\right) = \textbf{ceiling}\left(\frac{2fL}{c}\right), \tag{18}$$

where $L = W$ if a mode is in the x-direction and $L = H$ if a mode is in the y-direction. W is set to 0.8 m, which allows minimum 5 cut-on modes and maximum 14 cut-on modes (only counting the non-negative ones) in the frequency range of interest in the x-direction according to equation (18). H is set to 4.5 cm which only allows the 0^{th} mode in the y-direction.

3.2. Optimization of microphone locations

The number of microphone locations s is set to 30, which ensures $s > 2N$ (i.e., number of microphone locations per side larger than twice the number of cut-on modes) in the entire frequency range of interest. The goal of the optimization study is to define 30 microphone locations at each side of the sample. First, the frequency range of interest is sub-divided into several frequency bands, separated by the cut-on frequencies. The cut-on frequency of the m^{th} mode f_u^c is calculated as:

$$f_u^c = \frac{mc}{2W}, \tag{19}$$

where m takes an integer value between 0 and $N-1$. The intention of creating multiple frequency bands is to give higher priority to a higher frequency since according to equation (18) there exist more cut-on modes at a higher frequency which makes the measurement less over-determined.

Given the fact that the condition number becomes infinite at frequencies where modes become cut-on, frequency points between 1 Hz before each cut-on mode and 10 Hz after each mode are ignored. Thus the frequency range of the u^{th} band is $\left[f_{u-1}^c + 10 \text{ Hz}, f_u^c - 1 \text{ Hz}\right]$, where f_u^c is the u^{th} cut-on frequency in the frequency range of interest. The frequency range for the 1^{st} and the last frequency band within the range are [1000 Hz, $f_1^c - 1$ Hz] and $[f_{\text{last}}^c + 10 \text{ Hz}, 3000 \text{ Hz}]$, where f_{last}^c is the last cut-on frequency within the range and f_1^c is the first cut-on frequency within the range.

Next, for each frequency band, a linear average of the condition number of the modal matrix $\underline{M}$ is calculated, denoted as $\overline{\mathbf{cond}\left(\underline{M}\left(x,z,f\right)\right)}_u$ for the u^{th} frequency band.

Moreover, a weighting factor $w_u\left(f\right)$ is assigned to each frequency band, which is defined as:

$$w_u\left(f\right) = \frac{1}{N\left(3000 \text{ Hz}\right) - N_u}, \tag{20}$$

where N_u represent the number of cut-on modes at the u^{th} frequency band.

The objective function $F\left(x,z\right)$ which is the weighted average of linear averages for all frequency bands is calculated as:

$$F\left(x,z\right) = \sum_{u=1}^{Q} w_u\left(f\right) \overline{\mathbf{cond}\left(\underline{M}\left(x,z\right)\right)}_u, \tag{21}$$

where Q is the number of frequency bands with the frequency range of interest.

Since 60 variables (x, z values of 30 microphone locations) are required in the optimization, a great number of local minima is expected. A specific initial layout is chosen instead of a random layout to ensure a good starting point. Two lines of evenly distributed points are known to result in a reasonable condition number over a broad frequency range and are therefore selected as the initial layout for the optimization. A spacing of 4 cm between the two lines is chosen based on a numerical study of the condition number of the modal matrix in the frequency range of interest for a layout of two lines with a spacing ranging from 2 cm to 7 cm.

In the optimization of the microphone locations, points that are within 1 cm to the two side boundaries and 4 cm to the top, bottom boundaries of the waveguide and 4 cm to the sample region surfaces are excluded. The intention is to avoid inaccurate measurements close to boundaries or discontinuities. The initial layout and the optimized layout are shown in the left figure of Figure 3. Right figure of Figure 3 presents the condition number of the modal matrix as a function of frequency for the initial and optimized microphone layout. It is clear that he optimization successfully improves the condition number of $\underline{M}$ in the full range between 1000 Hz and 3000 Hz.

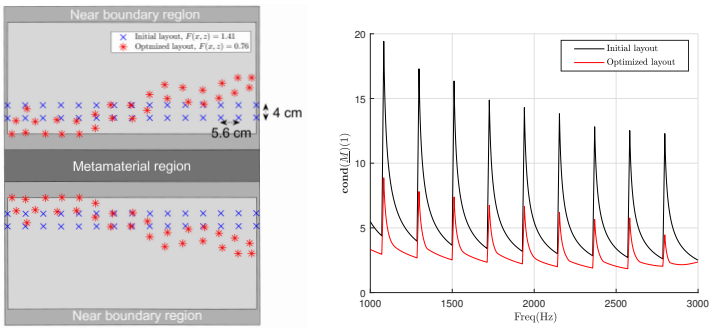

Figure 3: Left: Microphone layouts. Blue cross - original layout. Red asterisk - optimized layout. For each layout, the parts below and above the metamaterial are symmetric; Right: The condition number of the modal matrix as a function of frequency for the initial layout (black) and the optimized layout (red)

4. Numerical and experimental study

The methodology mentioned in section 2 and 3 is applied to both simulation of a waveguide where an acoustic metamaterial sample is placed inside and the corresponding experimental measurements of the same waveguide with the same type of metamaterial. This section describes the metamaterial used, the numerical and experimental setups and results.

4.1. Description of the metamaterial

The metamaterial design is based on the generalized Snell's law such that the absorption of a poroelastic (PE) material can be enhanced. It is composed of cells separated by metallic plates, where each cell is composed of an air layer at the top, a PE layer in the middle and another air layer at the bottom. A schematic illustration can be found in Figure 4. The PE material properties are measured in an impedance tube using the two cavity method [9]. Based on these properties, analytical models can be used to predict the phase of reflection and transmission coefficients of each cell, which can then be used to make the design, where the PE layer thickness and location is varied in each cell to form a phase gradient at both the top and the bottom surfaces. With two phase gradients, according to the generalized Snell's law, the absorption can be enhanced. Details of the process can be found in paper [10].

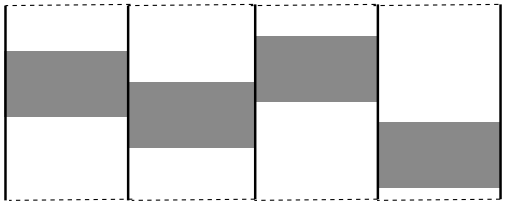

Figure 4: Schematic representation of a period composing of four cells. White: air layer; Gray: poroelastic layer

4.2. Numerical setup

A model of the waveguide is created in COMSOL Multiphysics® with the dimensions and the optimized layout described in section 3. As shown in Figure 5, a sample of the previously described anisotropic metamaterial is placed inside the virtual waveguide. The number of measurements w is set to 32 to satisfy $w > 2N$, which results in a fully or overly determined group of equations when calculating the scattering matrix (equation (13)). The number of measurements w should not be confused with the number of microphone locations s. Different measurements are performed by varying the sound source location on two ends of the waveguide, as is also shown in Figure 5. The distribution of sound source locations at each side is not symmetric in terms of the duct axis to avoid redundacies during the measurement since two symmetric sound source locations can be approximately regarded as two identical excitations.

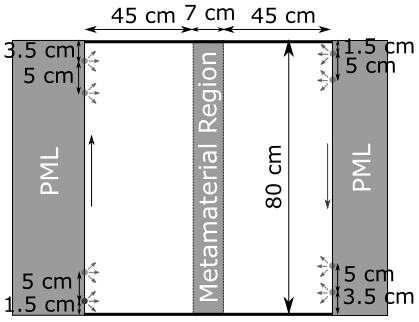

Figure 5: Numerical model for the waveguide simulation. 32 sound source locations (measurements) are used with 16 on top and 16 at the bottom.

As a comparison, the same metamaterial under plane wave incidence is simulated in an idealized manner considering: 1) plane wave incidence with different angles of incidence, 2) a semi-echoic termination (a perfectly matched layer both above and below the sample region) and 3) the structure is of infinite extent in the lateral direction (a periodic boundary condition both to the left and the right of the sample). This case is denoted as idealized plane wave incidence case (IPWI).

For the simulations of the waveguide under different sound source locations, after the acoustic pressure at points dictated by the optimized layout are obtained, procedures described in section 2 are followed so that R_o and T_o that correspond to IPWS case of the metamaterial can be calculated. The process of simulation of the waveguide and applying the measurement methodology to the simulation results afterwards is denoted as WGS.

4.3. Experimental setup

The waveguide with the optimized microphone layout is manufactured, as shown in Figure 6. A horn driver, whose position is varied between the measurements, is used as the sound source. Given the large number of microphone locations and the limited number of microphones available, at each sound source location, two submeasurements are performed covering different microphone locations. During each submeasurements, unused microphone locations are sealed by a dummy which is flushed with the inner surface of the top plate. The two submeasurements are then merged in the post-processing to give a complete measurement. Table 1 lists the details of the experimental setup. After obtaining the acoustic pressure at the prescribed points under different sound source locations, a similar procedure is followed as described in section 4.2 to obtain the R_o and T_o corresponding to the IPWI case.

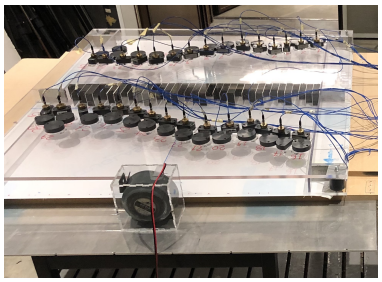

Figure 6: The experimental measurement setup. 8 periods of the metamaterial are used.

Parameter	Value
Number of microphone locations (each side)	30
Number of measurements	32
Number of submeasurements per measurement	2
Type of signals measured	acoustic pressure
Type of post-processing	Frequency response function (FRF)
Excitation signal	White noise
Sampling frequency	16384 Hz
Number of averages (for FPF calculation)	100
Overlap of adjacent windows (for FRF calculation)	50%

Table 1: Details of the experimental setup

4.4. Discussion of the numerical and experimental results

Figure 7 shows the reflection coefficient R, transmission coefficient T and absorption coefficient α directly measured from the experiment, obtained by applying the measurement procedure to the results of the

simulation of the waveguide and directly from the IPWI simulation of the metamaterial. A good match between the IPWI simulation and results of applying the measurement methodology to the WGS is found in both cases. For the normal incidence case, the mismatch around 1000 Hz and around 1500 Hz is due to the fact that the modal matrix is singular by definition at a cut-on frequency where the pressure field cannot be decomposed into modes. This is a limitation of the measurement method. From the oblique incidence absorption curve, one can see that, contrary to a continuous curve from the IPWI simulation, the WGS method only yields results at discrete angles. This is because at a certain frequency only a limited number of cut-on modes is present in a waveguide of finite dimensions, as can be seen from equation (18).

Results from the WGS generally match better with the IPWI simulation, as compared to the experimental measurement. The slight mismatch between the experimental measurement and the IPWI simulation is explained by the possibly inaccurate material characterization in the impedance tube using the two cavity method.

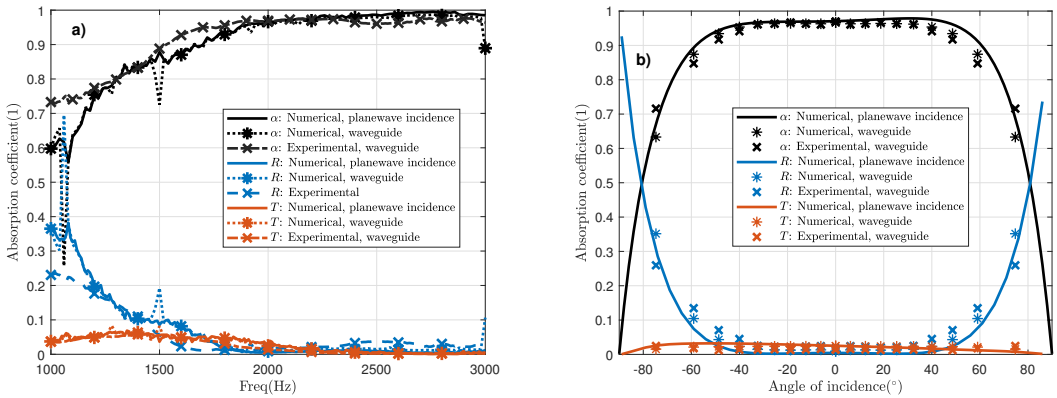

Figure 7: R, T and α of a metamaterial from both plane wave incidence simulation and applying the measurement methodology to the WGS under a) normal incidence, b) oblique incidence at 2000 Hz.

Additionally, as can be observed in Figure 8, the R_o and T_o of this material are not symmetric although the differences are small. For example, R_o under 60° incidence is not the same as that under −60° incidence. Contrarily, the R_o and T_o from the WGS are symmetric. This is because according to the modal decomposition theory, all mode shapes are symmetric, which means the pressure which is considered as a superposition of all cut-on modes will also always be symmetric. Thus, asymmetric materials cannot be accurately characterized using this method as no distinction can be made between two incidence angles of the same absolute value but different signs.

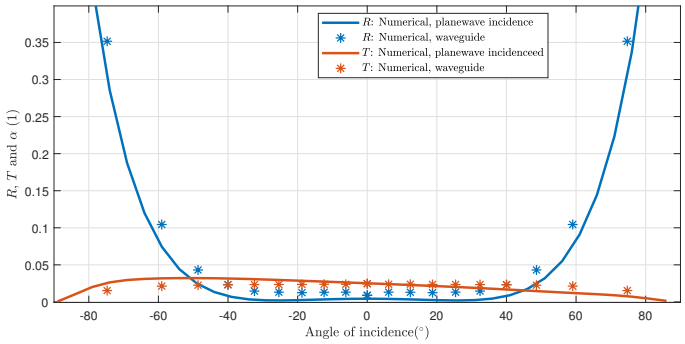

Figure 8: R, T of a metamaterial from plane wave incidence simulation and applying the measurement methodology to the WGS under oblique incidence at 2000 Hz. Figure zoomed in terms of the y-axis for readers' convenience.

5. Conclusions

A method to measure the oblique incidence reflection, transmission and absorption coefficients based on the modal decomposition theory in a rectangular waveguide is presented. The previously mentioned oblique incidence coefficients can be obtained from the corresponding coefficients of a certain mode, which can then be calculated using the modal decomposition method. The dimensions of the waveguide are chosen to avoid any high-order cut-on modes in one of the two directions of the cross-section and support multiple cut-on modes in the other direction of the cross-section. The intention is to ensure that the pressure field inside the waveguide can be represented by the acoustic pressure on one plane. An optimization on the microphone locations is performed to improve the robustness of the modal decomposition method and the accuracy of the measured metamaterial properties. The method is first validated by applying simulation results of a waveguide where a metamaterial sample is placed inside. The method is then applied experimentally on an anisotropic metamaterial sample inside the waveguide, where the results show a good agreement with the numerical predictions.

Acknowledgements

The research of Z. Zhang is funded by an Early Stage Researcher grant within the European Project PBNv2 Marie Curie Initial Training Network (GA 721615). Internal Funds KU Leuven are gratefully acknowledged for their support.

References

[1] E. Mommertz, Angle-dependent in-situ measurements of reflection coefficients using a subtraction technique, Applied Acoustics 46 (3) (1995) 251–263.
[2] C. Nocke, In-situ acoustic impedance measurement using a free-field transfer function method, Applied Acoustics 59 (3) (2000) 253–264.
[3] R. Lanoye, G. Vermeir, W. Lauriks, R. Kruse, V. Mellert, Measuring the free field acoustic impedance and absorption coefficient of sound absorbing materials with a combined particle velocity-pressure sensor, The Journal of the Acoustical Society of America 119 (5) (2006) 2826–2831.
[4] M. Müller-Trapet, M. Vorländer, In-situ measurements of surface reflection properties, Building Acoustics 21 (2) (2014) 167–174.
[5] M. Tamura, J. F. Allard, D. Lafarge, Spatial fourier-transform method for measuring reflection coefficients at oblique incidence. ii. experimental results, The Journal of the Acoustical Society of America 97 (4) (1995) 2255–2262.
[6] J. Prisutova, K. Horoshenkov, J.-P. Groby, B. Brouard, A method to determine the acoustic reflection and absorption coefficients of porous media by using modal dispersion in a waveguide, The Journal of the Acoustical Society of America 136 (6) (2014) 2947–2958.
[7] H. Denayer, Flow-acoustic characterization of duct components using multi-port techniques, Ph.D. thesis, KU Leuven, Dept. of Mechanical Engineering (2017).
[8] Angle-dependent reflection, transmission and absorption coefficients measurement using a 2d waveguide, Applied Acoustics 177 (2021) 107946.
[9] H. Utsuno, T. Tanaka, T. Fujikawa, A. Seybert, Transfer function method for measuring characteristic impedance and propagation constant of porous materials, The Journal of the Acoustical Society of America 86 (2) (1989) 637–643.
[10] Z. Ze, E. Deckers, C. Claeys, H. Denayer, W. Desmet, Absorption enhancement by phase gradient metamaterial, in: Forum Acusticum, 2020, pp. 2285–2290.